Talanta 130 (2014) 148–154

Contents lists available at ScienceDirect

Talanta

journal homepage: www.elsevier.com/locate/talanta

Excitation-emission matrix fluorescence coupled to chemometrics for the exploration of essential oils

William Mbogning Feudjio [a,b,*], Hassen Ghalila [b], Mama Nsangou [c], Yvon G. Mbesse Kongbonga [b], Youssef Majdi [b]

[a] Centre de Physique Atomique Moléculaire et d'Optique Quantique (CEPAMOQ), Faculty of Science, University of Douala, P.O. Box 8580, Douala, Cameroon
[b] Laboratoire de Spectroscopie Atomique Moléculaire et Applications (LSAMA), Faculty of Science, University of Tunis El Manar, P.O. Box 2092, Tunis, Tunisia
[c] University of Maroua, P.O. Box 46, Maroua, Cameroon

ARTICLE INFO

Article history:
Received 26 April 2014
Received in revised form
19 June 2014
Accepted 20 June 2014
Available online 30 June 2014

Keywords:
Excitation-emission matrix fluorescence
Essential oils
Unfold principal component analysis
Parallel factor analysis

ABSTRACT

Excitation-emission matrix fluorescence (EEMF) coupled to chemometrics was used to explore essential oils (EOs). The spectrofluorometer was designed with basic and inexpensive materials and was accompanied by appropriate tools for data pre-treatment. Excitation wavelengths varied between 320 nm and 600 nm while emission wavelengths were from 340 nm to 700 nm. Excitation-emission matrix (EEM) spectra of EOs presented different features, revealing the presence of varying fluorophores. EOs from the same species but from different origins presented almost the same spectra, showing the possibility that EEM spectra could be used as additional parameters in the standardisation of EOs. With the aid of unfold principal component analysis (UPCA), resemblances obtained by spectral analysis of EOs were confirmed. A five components parallel factor analysis (PARAFAC) model was used to find the profiles of fluorophores in EOs. One of those components was associated to *chlorophyll a*.

1. Introduction

Essential oils (EOs) are complex mixtures of volatile compounds produced by living organisms and isolated by physical means (pressing and distillation) from a whole plant or part of plant with known taxonomic origin [1]. Due to their beneficial biological properties (antimicrobial, antiviral, anti-oxidative, anti-fungal …), EOs are widely used in food, perfumes and pharmaceutical products [2]. That is why many efforts are made to regulate their production and distribution. In this context, the International Organization for Standardization (ISO) defines, in its technical committee (TC) 54, some standards for EOs [3,4]. For the analysis of EOs, chromatography is the most popular method [5] while few studies have reported the use of fluorimetry [6,7]. However, since components of EOs – terpenoids being major components of EOs – are most often characterised by the presence of a delocalised electron in their molecular structures, their absorption properties may be significant. Consequently, there might be a possibility for some of those components to possess fluorescence properties. This selective nature of fluorescence can be taken as an advantage for the discrimination of EOs and fluorescence spectra of EOs could be used as additional elements in the standardisation process of EOs. Moreover, the non-destructive nature of fluorescence and its avoidance of consumable reagents make it suitable for exploration purposes.

Due to the intrinsic broad nature of a fluorescence spectrum, conventional fluorescence offers a weak selectivity in the analysis of complex samples. In order to improve that selectivity, Johnson and co-workers developed the so-called excitation-emission matrix fluorescence (EEMF) whose spectra are presented in two dimensions [8]. EEMF has been successfully applied for the study of polycyclic aromatic hydrocarbons [9,10], vegetable oils [11,12] and dissolved organic matter [13,14]. There are standard instruments for EEMF's measurements such as the FluoroMax-3 (Jobin Yvon, France), the LS 50B (Perkin Elmer, United States) and the Cary Eclipse (Varian, United States) [15,16]. However, those instruments are not always accessible to some research units. Instead, basic materials that compose them might be available. Those materials could therefore be arranged according to EEMF's principles in order to allow reliable and accurate EEMF measurements.

The 2D character of EEMF spectra implies a three-way nature for a set of samples which can be analysed by adequate chemometric methods. Chemometrics has gained great popularity in the field of EEMF due to its usefulness in analysing large volumes of data [17].

The design of a simple spectrofluorometer, accompanied by appropriate data pre-treatment tools, for the exploration of EOs is

* Corresponding author at: Centre de Physique Atomique Moléculaire et d'Optique Quantique (CEPAMOQ), Faculty of Science, University of Douala, P.O. Box 8580, Douala, Cameroon. Tel.: +237 90 24 99 30/+216 24 14 28 37.
E-mail address: mbogningfeudjio@gmail.com (W. Mbogning Feudjio).

http://dx.doi.org/10.1016/j.talanta.2014.06.048
0039-9140/

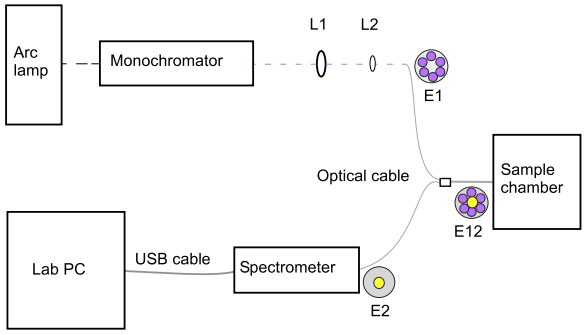

Fig. 1. Top view of the designed spectrofluorometer.

described in this study. The use of unfold principal component analysis (UPCA) and parallel factor analysis (PARAFAC) respectively to search patterns between EOs and to resolve the profiles of fluorophores present in EOs is also discussed.

2. Experimental

2.1. Apparatus

With simple and low cost materials, a spectrofluorometer was designed. The instrument is presented in Fig. 1.

The light source was a 150 W low cost Xenon arc lamp (Abet Technologies) which produces a continuous beam from 200 nm to 2000 nm. The excitation monochromator was a small H20 Vis (focal length 200 mm) of Jobin Yvon equipped with a mechanical counter. This monochromator allows excitation lines from 300 nm to 800 nm with a regular full width at half maximum (FWHM) of 8 nm. From the exit slit of the monochromator, the excitation beam was focused by two lenses L1 (calcium fluoride, diameter 5 cm, focal length 15 cm) and L2 (silica, diameter 2.5 cm, focal length 5 cm) onto the extremity E1 of the first leg of a UV–visible Y-type optical cable (Ocean Optics). This first leg is composed of six optical fibres (core diameter of 400 μm for each fibre) which brought the excitation light toward the sample's cell. The cell was installed in a home-made sample chamber and the excitation light illuminated it at an angle of 45°. The fluorescence light was collected at the extremity E12 of the cable by another optical fibre (core diameter 400 μm) surrounded by the six previous fibres. This optical fibre conducted the fluorescence light toward a spectrometer (USB 2000, Ocean Optics) connected at the extremity E2 of the second leg of the optical cable. Spectra were recorded with the software OOIBase32 (Ocean Optics). The use of a Y-type optical cable reduced inner filter effects since the absorbed light and the emitted light had the same path lengths [18].

In this study, the excitation wavelength range was set between 320 nm and 600 nm. In order to minimise redundancy and loss of information between emission spectra obtained with consecutive excitation wavelengths, in regard to the FWHM of excitation lines, a step of 10 nm was found appropriate for the excitation wavelength range. Thus, for each sample 29 emission spectra were to be recorded.

2.2. Samples and analysis

Fourteen EOs produced in Tunisia were considered in this study. Three mixtures of some of those EOs were also made. Samples are presented in Table 1.

The three samples of rosemary were produced in three different regions. The sample of schinus 1 was produced from leave of schinus. Schinus 2 was produced from unripe fruits of schinus and finally schinus 3 was produced from ripe fruits of schinus.

Table 1
Samples of EOs. For mixtures, the first term in bracket indicates the codes of the two EOs involved in the mixture; the second term in bracket gives their relative volume amount.

Code	EO	Species	Number of replicates
1	Thyme	*Thymus vulgaris*	0
2	Mint	*Mentha piperita*	3
3	Myrtle	*Myrtus communis L.*	3
4	Neroli	*Citrus aurantium L.*	1
5	Orange	*Citrus sinensis*	3
6	Rosemary 1	*Rosmarinus officinalis L*	1
7	Rosemary 2	*Rosmarinus officinalis L*	1
8	Rosemary 3	*Rosmarinus officinalis L*	1
9	Schinus 1	*Schinus terebinthifolius*	1
10	Schinus 2	*Schinus terebinthifolius*	0
11	Schinus 3	*Schinus terebinthifolius*	0
12	Wormwood	*Artemisia absinthium L.*	3
13	Lavender	*Lavandula angustifolia*	3
14	Ginger	*Zingiber officinalis*	2
15	Mixture 1=(4+8) (1:100)	–	0
16	Mixture 2=(12+8) (5:2)	–	0
17	Mixture 3=(4+12) (1:75)	–	0

Samples were stored in vials at a mean temperature of 20 °C. For the analysis, a volume of 0.5 mL of each sample was put in a quartz mini cell (volume 1.5 mL, path length 10 mm) and 29 emission spectra were recorded consecutively. A dark spectrum corresponding to the thermal background of the detector was also recorded. When needed, because EOs are strongly odorous and hydrophobic, mini cells were dipped in ethanol for one day before they were cleaned and rinsed with water.

2.3. Data pre-treatment

2.3.1. Correction of instrumental biases

For each sample, the dark spectrum was subtracted to each of the 29 emission spectra. After that, the correction of the spectrometer's sensitivity was performed. That correction was made by dividing each emission spectrum by correction factors of the spectrometer. To get those correction factors, we took advantage on the software OOIBase32 for its ability to compute the spectrum of a black body light source of known colour temperature [19]. The correction factors were obtained by the ratio between the experimental spectrum (spectrum of the black body light source recorded by the spectrometer) and the theoretical spectrum (spectrum of the black body light source computed by OOIBase32). A classical incandescence lamp was used as the black body light source. Because its colour temperature was not known, several temperatures between 2400 K and 3000 K by step of 100 K were tested. Each of them gave rise to particular correction factors. In order to choose the true correction factors, the same task was performed for the incandescence lamp with another spectrometer (USB 4000, Ocean Optics) in the same experimental conditions as for the USB 2000 spectrometer. Then, emission spectra, of rosemary 3 EO, obtained with both spectrometers at the excitation wavelength 370 nm were corrected with each set of correction factors. After that, the corrected spectra of rosemary 3 EO obtained for both spectrometers were compared for each set of correction factors. The correction factors corresponding to the colour temperature 2700 K were found to be the correct ones. Fig. 2 presents the spectra obtained for rosemary 3 EO before and after correction by correction factors corresponding to 2700 K.

The uncorrected spectra in (a) were recorded in the same conditions. Only the spectrometer was changed. After being corrected for the spectrometer sensitivity, the corrected spectra in (b) were

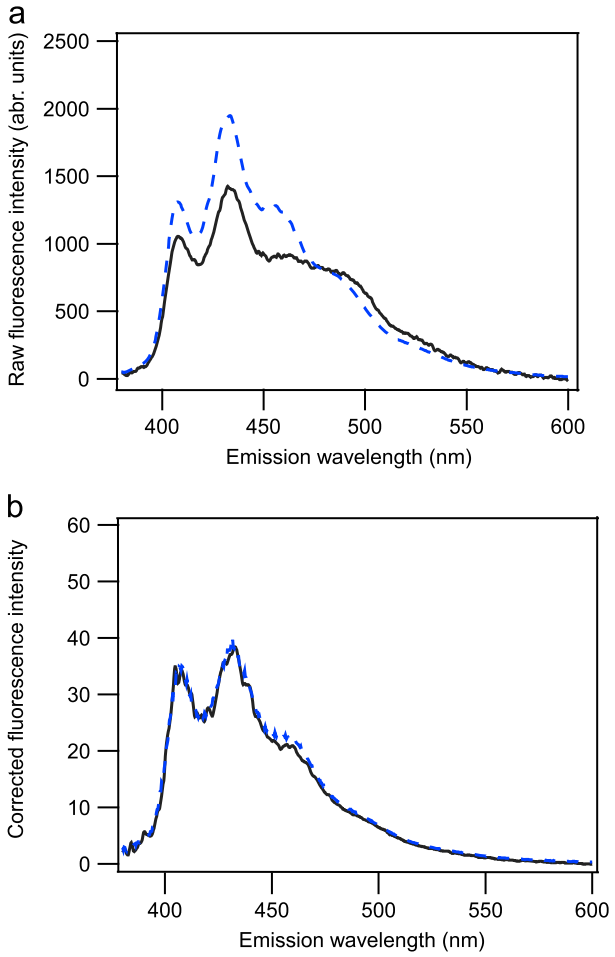

Fig. 2. Fluorescence spectra of rosemary 3 EO obtained at excitation wavelength 370 nm with USB 2000 (dashed line) and USB 4000 (solid line): (a) raw spectra; (b) corrected spectra.

almost identical. The Pearson's correlation coefficient between the two spectra was 0.9988, which validates the correction approach. This simple procedure for the correction of the bias due to the sensitivity of the spectrometer was a low cost alternative to the use of a radiometric light source.

Finally, the correction of the efficiency of the excitation compartment (arc lamp plus monochromator) was made. For that purpose, the extremity E12 of the optical cable was directly placed in front of the spectrometer and the integration time of the camera was set to a value (10 ms) for which signals were on scale (all signals were detected and there was no signal saturation). Then, for each of the 29 excitation wavelengths, the corresponding spectrum was recorded. Each of those 29 spectra was then corrected for the bias due to the sensitivity of the spectrometer. After that correction, the area of each corrected excitation peak was proportional to the intensity delivered by the excitation compartment and was subsequently used as correction factor. For each excitation wavelength, the correction was made by the ratio between the corresponding emission spectrum and the corresponding peak area. This simple approach for the correction of the bias due to the efficiency of the excitation compartment was a low cost alternative to the use of a quantum counter. For both corrections (sensitivity of the spectrometer and efficiency of the lamp plus the monochromator), an assumption was made that there was no energy transfer between fluorophores and that each fluorophore absorbed light independently of others.

2.3.2. Removal of scattering

Emission spectra were affected by the Rayleigh scattering. There were no features corresponding to the Raman scattering. The Rayleigh scattering was prominent due to the use of the Y-type optical cable. Mini cells were the main cause of that scattering. Since such scattering does not contain useful information in regard to EEMF, it was removed in a manner almost similar to the one described by Braham et al. [20]. For each emission spectrum, a window of 30 nm centred at the excitation wavelength used was set to missing. Then, a linear interpolation was made to the area set to missing. Others parts of the spectrum remained unchanged.

After the removal of the scattering, the emission wavelength range was set between 340 nm and 700 nm. Then, a cubic spline interpolation was made to the whole spectrum in order to reduce the number of wavelengths describing the spectrum from 1003 wavelengths to 200 wavelengths with a step of 1.8 nm. The aim of that reduction was principally to speed the data analysis step. After that, all the 29 emission spectra were concatenated and rearranged to produce the corresponding EEM of dimension 200×29. The entire data pre-treatment step was programmed and implemented with the software Igor Pro 6.0 which was also used for graph plotting.

3. Theory

3.1. Unfold principal component analysis (UPCA)

The purpose of UPCA is to matricize a three-way array and then perform a principal component analysis (PCA) [12,18,21]. PCA reduces the dimension of observation of large data by searching the latent variables which describe the highest variability in the data.

3.2. Parallel factor analysis (PARAFAC)

A three-way data of dimension $I \times J \times K$ can be analysed by PARAFAC in order to find the profiles of fluorophores present in samples [9,10,22,23]. I represents the dimension of the sample mode, J is the dimension of the emission mode and K is the dimension of the excitation mode. Fluorophore's profiles can be well resolved if two conditions are fulfilled. Firstly, the three-way data must conform to a three linear structure. Assuming here that absorbances of EOs were small, this first criterion was considered fulfilled because the non-three linear part (Rayleigh) had been removed and since an assumption had been previously made on the independence of each fluorophore. Secondly, fluorophores in samples must vary adequately in term of concentration. For this last criterion, since fluorophores were unknown, it was assumed that if fluorophores are present in EOs, their concentrations must not be predictable from one EO to another since EOs were independent. Mixtures of EOs were also taken into consideration to fulfil this criterion.

For a three-way array $\underline{\mathbf{X}}$, the purpose of PARAFAC is to decompose $\underline{\mathbf{X}}$ into components according to:

$$x_{ijk} = \sum_{f=1}^{F} a_{if} \times b_{jf} \times c_{kf} + e_{ijk}$$

x_{ijk} is an element of $\underline{\mathbf{X}}$ at position ijk. It represents the fluorescence intensity of sample number i at emission wavelength number j with the excitation wavelength number k. F is the number of components. a_{if}, b_{jf} and c_{kf} are respectively elements of **A**, **B** and **C** matrices. Columns of **A** account for concentrations of each fluorophore in the I samples; columns of **B** represent emission spectra (here described by J emission wavelengths) of fluorophores and columns of **C** represent excitation spectra (here described by K

excitation wavelengths) of fluorophores. e_{ijk} is the residual error for the element x_{ijk}. UPCA and PARAFAC are both fitted by alternative least square algorithms. The packages FactoMineR and ThreeWay of R.3.0.1 [24–26] were used respectively to perform UPCA and PARAFAC.

4. Results and discussion

4.1. EEM analysis of EOs

EEM spectra obtained for samples of EOs are presented in Fig. 3.

In the following, the position of a peak of maximum intensity will be written as Exc/Em, where Exc and Em state respectively for the excitation and emission wavelengths expressed in nanometre (nm).

In Fig. 3, the similitude between the spectra of thyme before (0) and after (1) Rayleigh removal shows that the approach for the treatment of the Rayleigh was good. Mint (2) is characterised by the presence of two peaks around 390/440 and 390/450. The same peaks are found in orange (5) and lavender (13). Those peaks may be related to fluorophores common to the three EOs. Additionally, orange presents a shoulder around 410/500 and lavender has another peak at 340/350. Myrtle (3) shows five narrowed peaks around 330/345, 355/385, 385/407, 385/433 and 385/459. Those peaks are also found in rosemary oils (6,7,8), meaning that common fluorophores might be present in myrtle and rosemary oils. All the rosemary oils present the same shape, feature which was expected since they were all produced from the same species in different regions. In rosemary 1 (6), another peak at 406/676 is also observed. This peak may be related to *chlorophylls* or to their degradation products. Neroli (4) presents a very different spectrum with a broad emission at 380/420 and a shoulder around 400/460. The spectra of schinus (9,10,11) are identical in the emission range from 350 nm to 625 nm. For schinus 1 (9), there is a strong emission of *chlorophylls* around 410/670. This emission confirms the fact that the raw material for schinus 1 was leaves of schinus. In wormwood (12), the strong variation of the wavelength of maximum emission with the excitation wavelength indicates the presence of many fluorophores. The same observation can be made for ginger (14). Thyme (1), wormwood (12) and ginger (14) present similar spectra.

EEM spectra of the fourteen EOs plus those of the three mixtures were arranged to produce the three-way array noted **Ar** of dimension $17 \times 200 \times 29$. EEM spectra of the fourteen EOs added to those of the three mixtures plus those of replicates of each EO were also arranged to produce the three-way array noted **Arr** of dimension $39 \times 200 \times 29$. The dimension of the sample mode in **Arr** is obtained by adding all the fourteen EOs, the three mixtures and the replicates (fourth column of Table 1).

4.2. UPCA of EOs

The array **Ar** was matricized on the sample mode. This gave a data matrix of dimension 17×5800. PCA was performed on that data matrix to look for patterns between EOs. The optimal preprocessing was column mean-centering without scaling or normalisation. Base on the precedent analysis of EEM spectra, four factors were retained. They explained 97.97% of the variation in the data. The positions of EOs in the two first principal component (PC) planes are shown in Fig. 4.

Fig. 4 shows in (a) how samples are gathered in the first principal component plane. The patterns observed confirm the observations made on EEM spectra. EOs of rosemary are regrouped in the cluster C1. Contrary to what was expected, myrtle (3) is far from C1. This feature might be the consequence of an underlying phenomenon presents in myrtle and not in rosemary or alternatively. All schinus EOs are clustering in C2. This means that PC1 and PC2 describe only the variation in the emission range from 350 nm to 625 nm. C3 confirms the resemblance between mint (2), orange (5) and lavender (13). The similitude between thyme (1), wormwood (12) and ginger (14) is confirmed by C4. Neroli (4) confirms its big difference by being far from the centre of the score plot and isolated from other EOs. In (b) the clustering becomes less evident because PC1 and PC3 explain less variation (76.68%) in the data as compare to PC1 and PC2 (85.38%). Schinus 1 (9) is clearly separated from schinus 2 (10) and schinus 3 (11). This means that PC3 describes the variation of the data including the emission region above 625 nm. Moreover the score of schinus 1 (9) along PC3 is very high as compared to the ones of other EOs. Thus, PC3 must be strongly related to *chlorophylls*. This feature is confirmed by rosemary 1 (6) which presents a slightly greater score on PC3 than rosemary 2 (7) and rosemary 3 (8).

4.3. PARAFAC of EOs

In order to resolve the profiles of fluorophores in EOs, the array **Arr** was fitted by a PARAFAC algorithm. **Arr** was mean centred across emission and excitation modes. Two, three, four, five, six and seven components models were tested. The explained variance for each number of components is given in Table 2.

According to Table 2, the relative change in explained variances becomes small above the three components model. On the other side, explained variances above the three components model are good. This is consistent with what was found in UPCA. In order to select the adequate number of components, a split half analysis was made on the four, five, six and seven components models and the behaviour of the loadings for each model was also examined. Two splitting approaches were tested: a random splitting and a splitting according to the position (odd or even) of each sample. Both splittings lead to similar results. The five components model was the most stable. Table 3 shows the stability of the estimates of the five components model.

Only component 4 was unstable. The profiles obtained by PARAFAC are shown in Fig. 5.

The first component has an emission profile with resolved peaks. Such behaviour can be related to a rigid molecular structure. On the contrary, the second and the third components are characterised by broad emission peaks, meaning that their vibrational levels might be active. The instability of component 4, found in Table 3, is confirmed by the feature of its emission spectrum. Excitation and emission spectra of component 5 correspond to those of *chlorophyll a* [27]. Scores of the five components are shown in Fig. 6.

Fig. 6 shows that neroli is the mixture of components 1, 2 and 3. Rosemary oils have a high amount of component 1. In G3, schinus 1 presents the highest amount of *chlorophyll a*. G4 shows that component 2 is representative in ginger.

5. Conclusion

The design of a simple spectrofluorometer with inexpensive materials has been described in this study. The spectrofluorometer was accompanied by appropriate tools for data pretreatment. The exploration of EOs by the spectrofluorometer has shown the possibility to use EEM spectra in the standardisation process of EOs. EEM spectra revealed the presence of different fluorophores in EOs and showed the possibility to describe them. UPCA has been used to find patterns between EOs and the ability of PARAFAC to resolve profiles of fluorophores in EOs has been discussed. In UPCA, EOs were gathered according

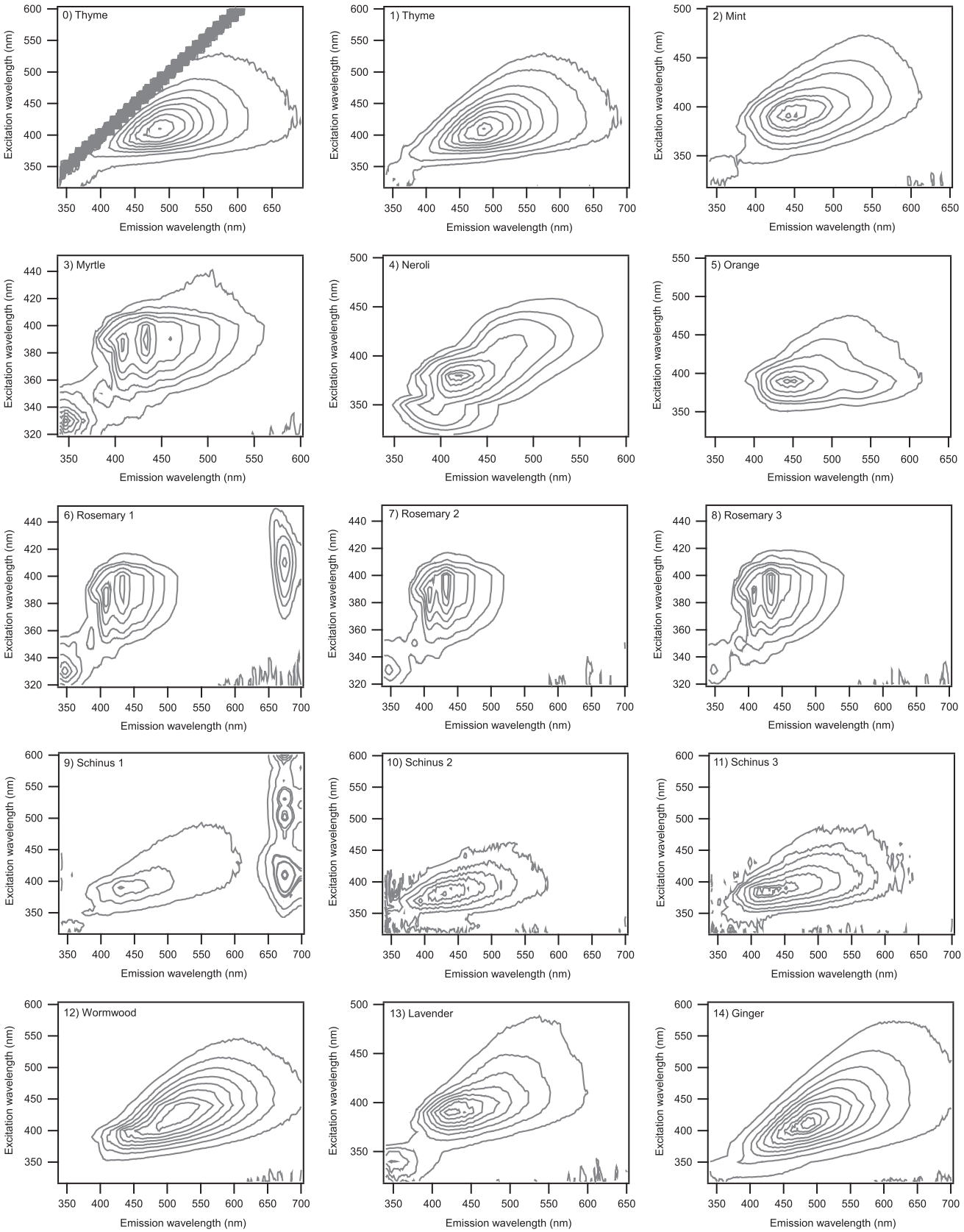

Fig. 3. EEM contour plots of EOs. For thyme, spectra with and without the Rayleigh scattering are shown. For each of the other EOs, the spectrum without the Rayleigh is presented.

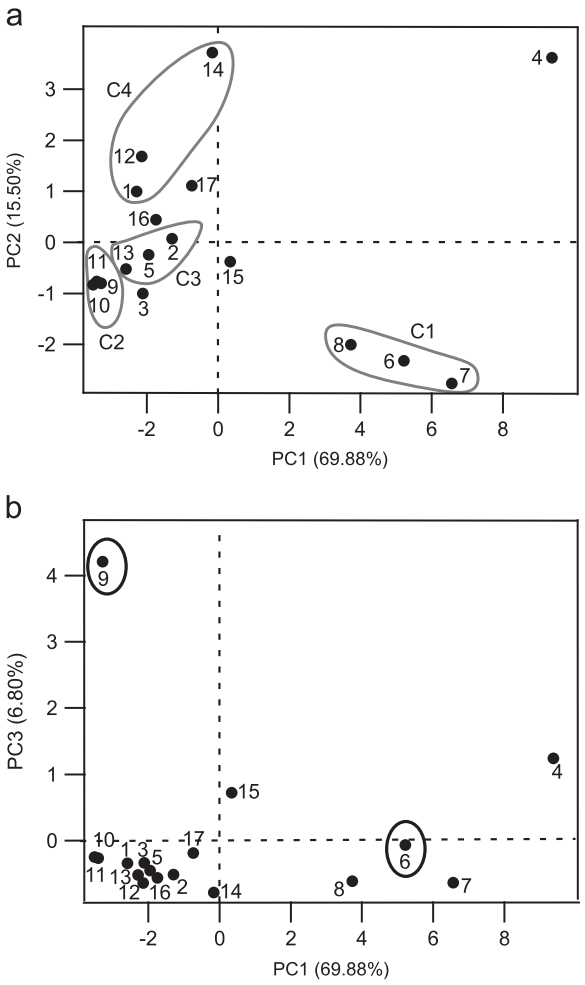

Fig. 4. Scores plots of EOs from UPCA: (a) first plane (PC1, PC2) with cumulative percentage of variance of 85.38%; (b) second plane (PC1, PC3) with cumulative percentage of variance of 76.68%.

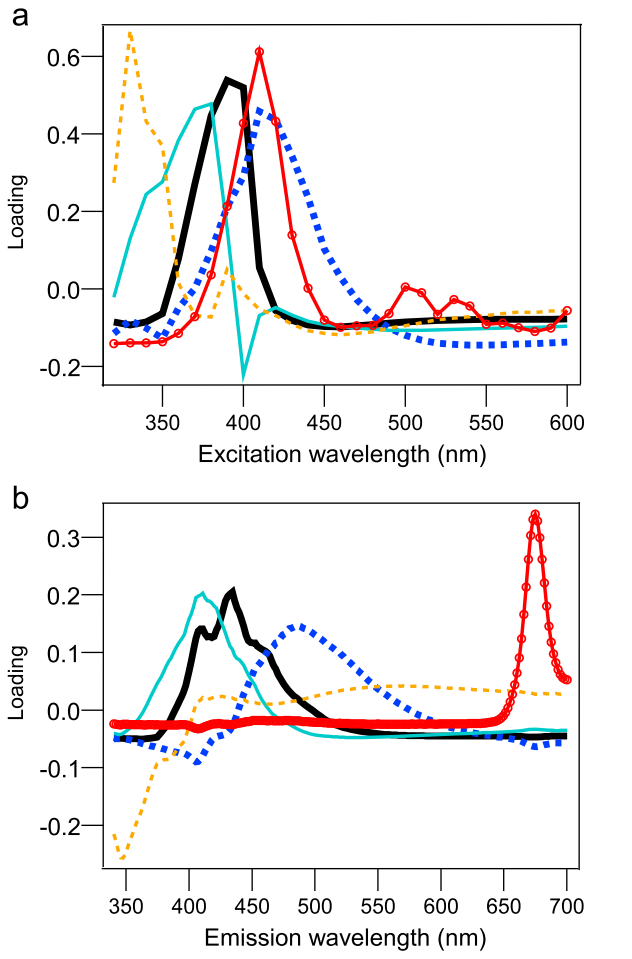

Fig. 5. Estimated profiles of fluorophores in EOs from PARAFAC: (a) excitation spectra and (b) emission spectra. Component 1: thick continuous line; component 2: thick dashed line; component 3: thin solid line; component 4: thin dashed line; component 5: thin line with circles.

Table 2
Explained variances in percentage (%) for the PARAFAC models.

Number of components	Two	Three	Four	Five	Six	Seven
Explained variance	82.48	88.22	92.31	94.75	96.66	97.85

Table 3
Split-half analysis results obtained for the five components model with the random splitting. I= correlations for samples in splits; II= congruence values for emission mode component matrix; III= congruence values for excitation mode component matrix.

Component	I		II	III
	Split 1	Split 2		
1	1.00	1.00	1.00	1.00
2	1.00	1.00	0.95	0.99
3	1.00	1.00	1.00	0.99
4	1.00	0.76	0.47	0.48
5	1.00	1.00	1.00	1.00

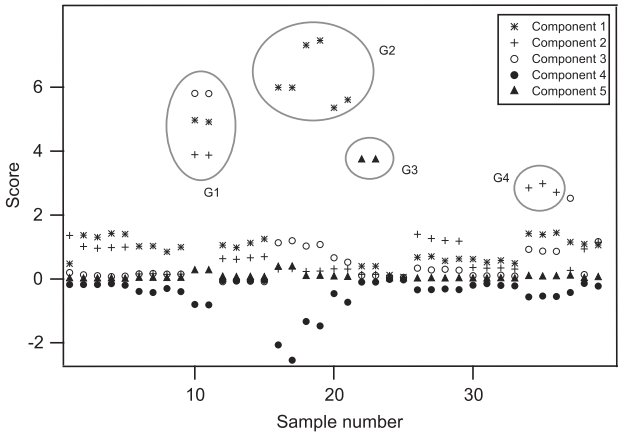

Fig. 6. Scores plot of EOs from PARAFAC. G1: neroli and its replicate; G2: rosemary and their replicates; G3: schinus 1 and its replicate; G4: ginger and its replicates.

to spectral resemblances. Among the five components resolved by PARAFAC, *chlorophyll a* was found. The identification of other fluorophores, which is a complex task, will be the subject of forthcoming works.

Acknowledgements

The authors are grateful to the Abdus Salam International Centre for Theoretical Physics (Italy) for financial support through NET – 45 and OEA – AC – 71 projects. They also acknowledge the Laboratoire Système de Production Agricole et Développement

Durable de l'Ecole Supérieure d'Agriculture de Mograne (Tunisia) and the company Carthago Essences (Tunisia) for providing them with samples of EOs. W. M. F. thanks Professors Zoubeida Dhaouadi, Nejm-Eddine Jaïdane, Souad Lahmar and Emeritus Professor Zohra Ben Lakhdar for providing the best conditions for the accomplishment of this work and for helpful discussions. Finally, the authors would like to thank anonymous reviewers for helpful suggestions.

References

[1] C. Franz, J. Novak, in: K.H.C. Başer, G. Buchbauer (Eds.), Handbook of Essential Oils: Science, Technology, and Applications, Taylor & Francis Group Inc., Boca Raton, 2010, pp. 39–81.
[2] G. Buchbauer, in: K.H.C. Başer, G. Buchbauer (Eds.), Handbook of Essential Oils: Science, Technology, and Applications, Taylor & Francis Group Inc., Boca Raton, 2010, pp. 235–280.
[3] ⟨http://www.iso.org/iso/home/standards_developement/list_of_iso_technical_committees⟩, (last accessed, 06.06.14.).
[4] A. Bordas, E. Bermejo, ISO Focus + 3 (2012) 12–13.
[5] B. d'A. Zellner, P. Dugo, G. Dugo, L. Mondello, in: K.H.C. Başer, G. Buchbauer (Eds.), Handbook of Essential Oils: Science, Technology, and Applications, Taylor & Francis Group Inc., Boca Raton, 2010, pp. 151–183.
[6] F. Boschi, M. Fontanella, L. Calderan, A. Sbarbati, Eur. J. Histochem. 55 (2011) 97–100.
[7] P. Giungato, L. Notarnicola, J. Commod. Sci. Technol. Qual. 44 (2005) 17–34.
[8] D.W. Johnson, J.B. Callis, G.D. Christian, Anal. Chem. 49 (1977) 747A–757A.
[9] R.D. JiJi, G.A. Cooper, K.S. Booksh, Anal. Chim. Acta 397 (1999) 61–72.
[10] O. Divya, A.K. Mishra, Anal. Chim. Acta 592 (2007) 82–90.
[11] E. Sikorska, A. Romaniuk, I.V. Khmelinskii, R. Herance, J.L. Bourdelande, M. Sikorski, J. Koziol, J. Fluoresc. 14 (2004) 25–35.
[12] F. Guimet, J. Ferré, R. Boqué, F.X. Rius, Anal. Chim. Acta 515 (2004) 75–85.
[13] P.G. Coble, Mar. Chem. 51 (1996) 325–346.
[14] B.J.H. Matthews, A.C. Jones, N.K. Theodorou, A.W. Tudhope, Mar. Chem. 55 (1996) 317–332.
[15] C. Goletz, M. Wagner, A. Grübel, W. Schmidt, N. Korf, P. Werner, Talanta 85 (2011) 650–656.
[16] R.M. Cory, M.P. Miller, D.M. McKnight, J.J. Guerard, P.L. Miller, Limnol. Oceanogr.: Methods 8 (2010) 67–78.
[17] K. Kumar, A.K. Mishra, Talanta 117 (2013) 209–220.
[18] H. Omrani, J.A. Barnes, A.E. Dudelzak, H.-P. Loock, H. Waechter, Analyst 137 (2012) 2782–2790.
[19] Ocean Optics, in: Ocean Optics (Ed.), OOIBase32, Spectrometer Operating Software. Installation and Operation Manual, Ocean Optics Inc., Dunedin Florida, 2005, pp. 61–74.
[20] M. Bahram, R. Bro, C. Stedmon, A. Afkhami, Handling of Rayleigh and Raman scatter for PARAFAC modeling of fluorescence data using interpolation, J. Chemom. 20 (2006) 99–105.
[21] S.M. Obeidat, T. Glasser, S.Y. Landau, D.M. Anderson, G.D. Rayson, Talanta 72 (2007) 682–690.
[22] R. Bro, Chemom. Intell. Lab. Syst. 38 (1997) 149–171.
[23] C.M. Andersen, R. Bro, J. Chemom. 17 (2003) 200–215.
[24] ⟨http://www.R-project.org/⟩, (last accessed 07.06.14.).
[25] ⟨http://factomineR.free.fr⟩, (last accessed 07.06.14.).
[26] P. Giordani, H.A.L. Kiers, M.A. Del Ferraro, J. Stat. Soft. 57 (2014) 1–23.
[27] L. Moberg, G. Robertsson, B.O. Karlberg, Talanta 54 (2001) 161–170.